Journal of Thermal Analysis, Vol. 32 (1987) 1151–1162

THERMAL DECOMPOSITION KINETICS OF SCHIFF BASE COMPLEXES OF COPPER(II) AND PALLADIUM(II)

V. Indira and *G. Parameswaran**

DEPARTMENT OF CHEMISTRY, UNIVERSITY OF CALICUT, INDIA 673 635

(Received May 20, 1986; in revised form September 17, 1986)

Thermogravimetric (TG), derivative thermogravimetric (DTG) and differential thermal analysis (DTA) curves of CuL_2 and $Pd(LH)_2Cl_2$ (LH = salicylidene-2-aminofluorene and 2-hydroxy-1-naphthalidene-2-aminofluorene) in air are studied. Mass loss considerations at the main decomposition stages indicate conversion of the complex to oxides. Mathematical analysis of TG data shows that first order kinetics are applicable in all cases. Kinetic parameters (energy and entropy of activation and preexponential factor) are reported.

Transition metal complexes of Schiff bases have important technical applications. Wendlandt [1–5] and Hill [6, 7] studied the thermal properties of metal chelates with different types of complexing ligands. Studies on thermal decomposition and kinetics of metal chelates with Schiff bases have been done by a few workers [8, 9]. In continuation of our work [10–12] on thermal decomposition kinetics of metal chelates, we report in this paper the thermoanalytical data of four complexes—copper(Ii) and palladium(II) complexes of the Schiff bases, salicylidene-2-aminofluorene (SAF) and 2-hydroxy-1-naphthalidene-2-aminofluorene (HNAF). Interpretation and mathematical analysis of those data and evaluation of order of reaction and the energy and entropy of activation, based on the differential method employing Freeman–Carroll equation [13], the integral method using the Coats–Redfern equation [14] and the approximation method using the Horowitz–Metzger equation [15] are also given. Zsakó's modified Doyle method [16] is also used for finding out energy and order of the reaction.

Experimental

The metal complexes of salicylidene-2-aminofluorene ($C_{20}H_{15}ON$) were prepared by refluxing 1*M* methanolic solution of the metal chloride and 2*M* methanolic solution of the ligand for about 10 hr. The metal complexes of 2-

John Wiley & Sons, Limited, Chichester
Akadémiai Kiadó, Budapest

hydroxy-1-naphthalidene-2-aminofluorene ($C_{24}H_{21}ON$) were prepared as follows. To an ethanolic solution of 2*M* 2-hydroxy-1-naphthaldehyde, 1*M* ethanolic solution of metal chloride solution was added, then warmed. To this 2*M* ethanolic solution of 2-aminofluorene was added and refluxed for about 14 hr. The precipitates were filtered, washed with the solvent used for preparation and dried in a vacuum desiccator. The structure of copper(II) and palladium(II) chelates was found to be of the formula CuL_2 and $Pd(LH)_2Cl_2$ respectively where LH = salicylidene-2-aminofluorene and 2-hydroxy-1-naphthalidene-2-aminofluorene [17].

Apparatus

TG and DTA curves were recorded on a Stanton recording thermobalance (Model TR 01) with a DTA attachment. The heating rates and other characteristics are given below: heating rate—4 deg min^{-1}, chart speed—3 in h^{-1}, atmosphere—static air, crucible (DTA(—platinum, reference substance—Al_2O_3. Buoyancy correction was applied.

Treatment of data

The instrumental TG curves were redrawn as mass *vs.* temperature (TG) curves and also as the rate of loss of mass *vs.* temperature (DTG) curves. The instrumental DTA curves were used as such. Typical TG, DTG, and DTA curves are presented in Figure 1 and the decomposition temperature ranges in DTA&DTG for the metal chelates are presented in Table 1.

The TG curves were studied in greater detail. The curves for all the four chelates exhibited a characteristic, well defined and non-overlapping decomposition pattern. The mass loss considerations and X-ray diffraction data indicated the products to be CuO and PdO. The relevant portion of the TG curve was redrawn on an expanded scale, using standard curve sets. Four different methods were used to evaluate kinetic data from these TG traces.

Differential method using the Freeman–Carroll equation [13]

The Freeman–Carroll equation was used in the form

$$\frac{\Delta \log \frac{dw}{dt}}{\Delta \log w_r} = \frac{(-E^*/2.303R)\,\Delta(T^{-1})}{\Delta \log w_r} \tag{1}$$

where $w_r = w_\infty - w$, w_∞ = mass loss at the completion of the reaction; w = mass loss upto time t; T = absolute temperature at time t; n = order of reaction; R = gas constant in cal and E^* = activation energy in J mol^{-1}. Of the above

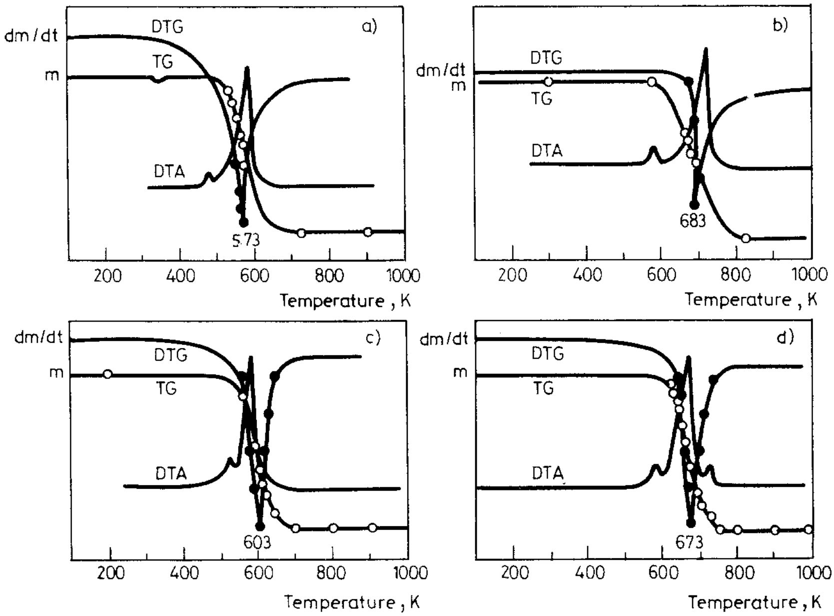

Fig. 1 TG, DTG and DTA curves of Pd(II) and Cu(II) chelates A = [Cu(SAF)$_2$], B = [Cu(HNAF)$_2$], C = [Pd(SAF)$_2$Cl$_2$], D = [Pd(HNAF)$_2$Cl$_2$]

terms, w_r and T can be directly obtained from the TG traces. The mass-temperature gradient ($\mathrm{d}w/\mathrm{d}T$) could be obtained by drawing tangents. The temperature slopes, $\mathrm{d}w/\mathrm{d}T$, were converted into time slopes, $\mathrm{d}w/\mathrm{d}t$ using the relation,

$$\frac{\mathrm{d}w}{\mathrm{d}t}=\left(\frac{\mathrm{d}w}{\mathrm{d}T}\right)\left(\frac{\mathrm{d}T}{\mathrm{d}t}\right)=\frac{\mathrm{d}w}{\mathrm{d}T}\varnothing \tag{2}$$

where $\varnothing$ is the heating rate. A plot of $\dfrac{\Delta T^{-1}}{\Delta \log w_r}$ *vs.* $\dfrac{\Delta \log(\mathrm{d}w/\mathrm{d}t)}{\Delta \log w_r}$ was drawn and found to be linear from which the order of reaction and activation energy were obtained from the intercept and slope, respectively. The order of reaction (n) was found to be nearer to unity. The usual first order rate law expression,

$$(\mathrm{d}x/\mathrm{d}t)=k(a-x) \tag{3}$$

can be put in the following form using the terms w and w_r

$$(\mathrm{d}w/\mathrm{d}t)=kw_r \tag{4}$$

combining this with Arrhenius equation, i.e.,

$$k=A\exp(-E^*/RT), \tag{5}$$

Table 1 Thermal decomposition data

Substance	Peak temperature in DTG, K	Temperature ranges in DTG, K	Peak temperatures in DTA, K	Temperature ranges in DTA, K	Loss of mass, %		
					From TG	Theoretical	From independent pyrolysis
$Cu(SAF)_2$	573 s	500–700	475 exo(w)	455–480	86.0	87.4	87.1
			573 exo(s)	500–700			
$Cu(HNAF)_2$	683 s	573–800	575 exo(w)	550–600	88.0	89.1	88.91
			683 exo(s)	600–750			
$Pd(SAF)_2Cl_2$	603 s	500–700	525 exo(w)	500–540	82.0	83.6	83.2
			603 exo(s)	540–650			
			585 exo(w)	550–600			
$Pd(HNAF)_2Cl_2$	673 s	500–750	673 exo(s)	600–710	84.0	85.5	84.9
			725 exo(w)	710–750			

we get

$$\log[(\mathrm{d}w/\mathrm{d}t)/w_r] = \frac{-E^*}{2.303RT} + \log A \tag{6}$$

A plot of the LHS of Eq. (6) against (T^{-1}) was found to be linear, from the slope of which E^* was calculated. A was calculated from the intercept and entropy of activation ΔS^* was obtained from the equation

$$A = \frac{kT}{h}\exp(\Delta S^*/R) \tag{7}$$

where k is the Boltzmann constant, h is the Planck constant and T_s is the peak temperature from DTG. Typical curves concerning the application of the Freeman–Carroll equation ($n = 1$) to all the chelates are given in Fig. 2.

Integral method using the Coats–Redfern equation [14]

Coats–Redfern equation, which is a typical integral method can be represented as

$$\int_0^\infty \mathrm{d}\alpha/(1-\alpha)^n = A/\varnothing \int_0^T \exp(-E^*/RT)\,\mathrm{d}t \tag{8}$$

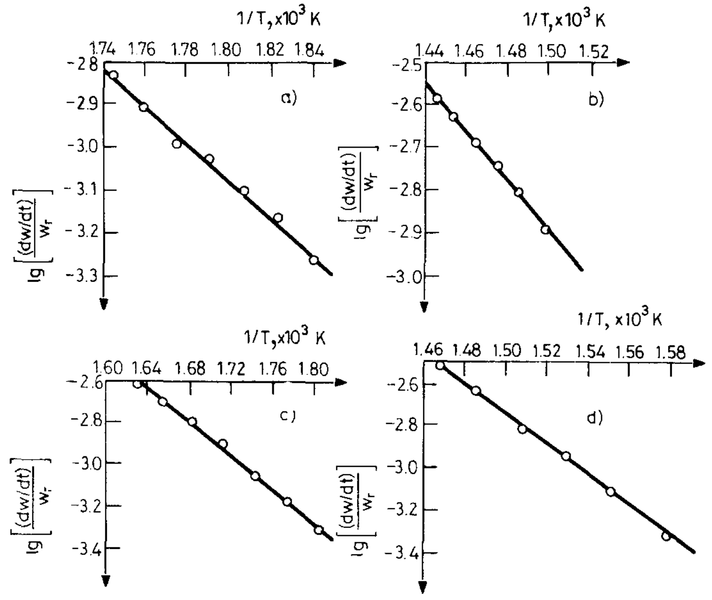

Fig. 2 Freeman–Carroll plots for the decomposition of Pd(II) and Cu(II) chelates. A = [Cu(SAF)$_2$] B = [Cu(HNAF)$_2$], C = [Pd(SAF)$_2$Cl$_2$], D = [Pd(HNAF)$_2$Cl$_2$]

The LHS of Eq. (8) has two different solutions, namely,

$$1-(1-\alpha)^{1-n}/(1-n) \quad \text{for } n \neq 1 \tag{9}$$

and

$$-\log(1-\alpha) \quad \text{for } n=1 \tag{10}$$

In both cases, the RHS of Eq. (8) has the solution

$$\frac{ART^2}{\varnothing E^*}\frac{(1-2RT)}{E^*}\exp(-E^*/RT) \tag{11}$$

Equation (12) and (13) are obtained after taking logarithms

$$\log\left[\frac{1-(1-\alpha)^{1-n}}{T^2(1-n)}\right] = \log\frac{AR}{\varnothing E^*}\frac{(1-2RT)}{E^*} - \frac{E^*}{2.303RT} \quad \text{for } n\neq 1 \tag{12}$$

and

$$\log\left[\frac{-\log(1-\alpha)}{T^2}\right] = \log\left[\frac{AR}{\varnothing E^*}\frac{(1-2RT)}{E^*}\right] - \frac{E^*}{2.303RT} \quad \text{for } n=1 \tag{13}$$

In ordinary thermal decomposition reactions, $\log\left[\frac{AR}{\varnothing E^*}\left(1-\frac{2RT}{E^*}\right)\right]$ is practically constant, and plots of

$$\log\left[\frac{1-(1-\alpha)^{1-n}}{T^2(1-n)}\right] \text{ vs. } 1/T \text{ for } n\neq 1 \tag{14}$$

and

$$\log\left[\frac{-\log(1-\alpha)}{T^2}\right] \text{ vs. } 1/T \text{ for } n=1 \tag{15}$$

respectively result in a straight line with a slope of $E^*/2.303R$ for the correctly chosen value of n. The reaction order can easily be estimated by observing the lines drawn by using $n=0.5$ and 0.67 in Eq. (14) and $n=1$ in Eq. (15). The application of Eqs (14) and (15) to our data on the copper(II) and palladium(II) chelates revealed that a better straight line results with Eq. (15) and hence the order of the reaction is unity.

For a first order process the Coats–Redfern equation may be written in the form

$$\log\left[\frac{\ln\frac{w_\infty}{w_\infty - w}}{T^2}\right] = \log\left[\frac{AR}{\varnothing E^*}\left(1-\frac{2RT}{E^*}\right)\right] - \frac{E^*}{2.303RT} \tag{16}$$

Since $1-\frac{2RT}{E^*}\simeq 1$, a plot of LHS of Eq. (16) against $1/T$ was drawn (Fig. 3). E^* was calculated from the slope and A was found from the intercept.

Approximation method using the Horowitz–Metzger equation [15]

The Horowitz–Metzger method is illustrative of the approximation methods. These authors derive the relation

$$\log\left[\frac{1-(1-\alpha)^{1-n}}{1-n}\right]=\frac{E^*\theta}{2.303RT_s^2}\quad \text{for } n\neq 1 \tag{17}$$

where $n=1$, the LHS of Eq. (17) would be $\log[-\ln/1-\alpha]$. For a first order kinetic process the Horowitz–Metzger equation may be written in the form

$$\log\left[\log\frac{w_\infty}{w_r}\right]=\frac{E^*\theta}{2.303RT_s^2}-\log 2.303 \tag{18}$$

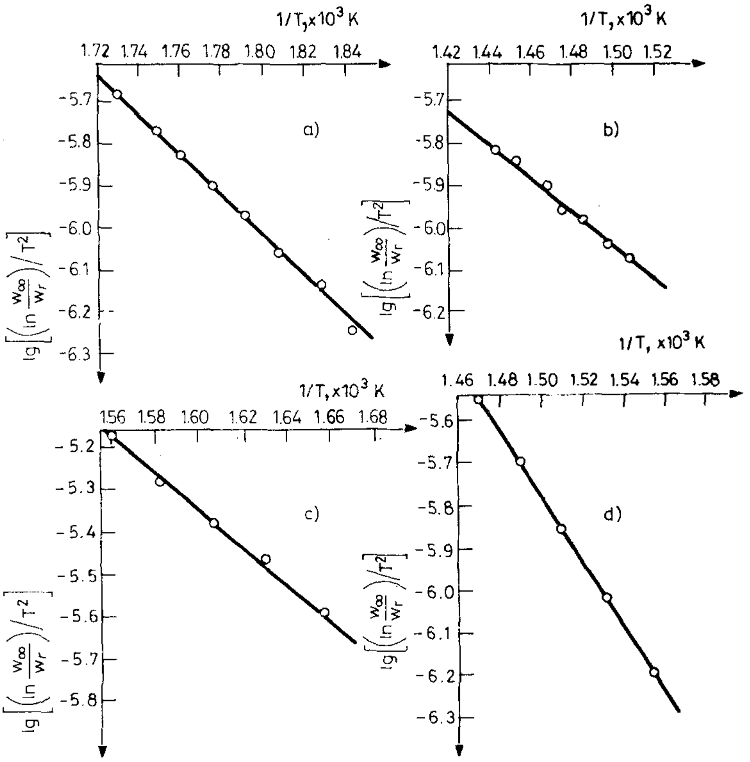

Fig. 3 Coats–Redfern plots for the decomposition of Pd(II) and Cu(II) chelates. A = [Cu(SAF)$_2$], B = [Cu(HNAF)$_2$], C = [Pd(SAF)$_2$Cl$_2$], D = [Pd(HNAF)$_2$Cl$_2$]

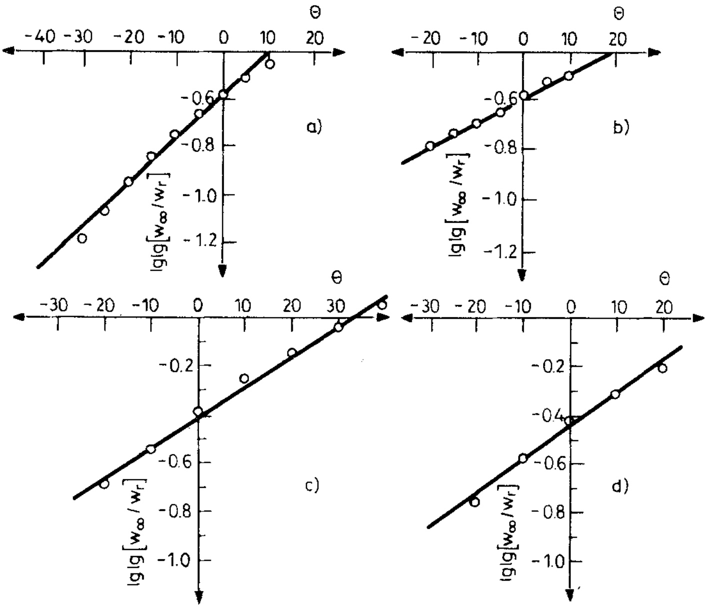

Fig. 4 Horowitz–Metzger plots for the decomposition of Pd(II) and Cu(II) chelates. A = [Cu(SAF)$_2$], B = [Cu(HNAF)$_2$], C = [Pd(SAF)$_2$Cl$_2$], D = [Pd(HNAF)$_2$Cl$_2$]

where $\theta = T - T_s$ and the other terms are as described earlier. A plot of log [log (w_∞/w_r)] *vs.* θ was drawn and was found to be linear from the slope of which E^* was calculated. Typical plots are given in Fig. 4. The preexponential factor A was calculated from the equation

$$\frac{E^*}{RT_s^2} = \frac{A}{\varnothing \exp(-E^*/RT_s)} \tag{19}$$

The entropy of activation ΔS^* was calculated from the Eq. (7) used earlier for the purpose.

Zsakó's modified Doyle method [16]

The trial and error method of Doyle was modified by Zsakó by introducing the standard deviation instead of curve fitting method for the calculations.

The value of $g(\alpha)$ was calculated for various values of 'n' in the general equation $\frac{d\alpha}{dt} = k(1-\alpha)^n$, where '$n$' can be considered as apparent reaction order. The values of 'n' taken are $n = 0$, 0.5, 1 or 2.

If the logarithm of Doyle's equation is taken,

$$\log AE^*/R\varnothing = \log g(\alpha) - \log P(x) = B \tag{20}$$

where $g(\alpha)$ is a certain function of α, where α stands for the fraction of initial compound reacted, A = frequency factor, E^* = activation energy, R = gas constant and $\varnothing$ = heating rate. The values of the integral

$$P(x) = \frac{e^{-x}}{x} - \int_{x}^{\infty} \frac{e^{-u}}{u} \mathrm{d}u \quad (\text{where } u = E^*a/RT) \tag{21}$$

were calculated and tabulated by Doyle for x values covering a range from 10 to 50 and these values were used in calculating 'B'. The average of B values, as obtained at different temperatures, was taken and $\partial = \frac{(Bi - \bar{B})^2}{r}$ where Bi is any value, $\bar{B}$ is arithmetical meon and r is number of values. ∂ values for various 'B' values are calculated and given in Table 2. The ∂ value is minimum if the apparent order of reaction n is taken as 1, i.e., first order reaction. Thus from tested 'n' values, $n = 1$ is the best.

Result and discussion

The decomposition temperature ranges in DTA and DTG, for the metal chelates are given in Table 1. Data from independent pyrolysis experiments (carried out by

Table 2 Zsakó's modified method ∂ values

Substance	E^*	$n=0$	$n=0.5$	$n=1$	$n=2$
$Cu(SAF)_2$	20	0.0011	0.0217	0.0001	0.0104
	22	0.0054	0.0235	0.0036	0.0667
	24	0.0010	0.0137	0.0047	0.0034
	26	0.0010	0.0174	0.0042	0.0002
$Cu(HNAF)_2$	20	0.0028	0.0482	0.0041	0.0109
	22	0.0065	0.0339	0.0005	0.0040
	24	0.0062	0.0218	0.0022	0.0017
	26	0.0105	0.0175	0.0147	0.0021
$Pd(SAF)_2Cl_2$	14	0.0007	0.0210	0.0026	0.0260
	16	0.0250	0.0212	0.0004	0.0229
	18	0.0307	0.0126	0.0027	0.0207
	20	0.0040	0.0135	0.0038	0.0195
$Pd(HNAF)_2Cl_2$	24	0.0097	0.0379	0.0062	0.0050
	26	0.0032	0.0278	0.0005	0.0292
	28	0.0307	0.0153	0.0062	0.0383
	30	0.0040	0.0474	0.0083	0.0186

Table 3 Kinetic data

Substance	Parameters	From Freeman–Carroll equation	From Coats–Redfern equation	From Horowitz–Metzger equation
$Cu(SAF)_2$	E^* (kJ mol^{-1})	87.0	91.2	104.8
	A (s^{-1})	1.25×10^5	2.68×10^5	9.11×10^6
	ΔS^* (JK mol^{-1})	−152.8	−146.46	−117.2
$Cu(HNAF)_2$	E^* (kJ mol^{-1})	95.4	76.6	89.3
	A (s^{-1})	5.98×10^4	5.63×10^2	1.03×10^4
	ΔS^* (JK mol^{-1})	−160.4	−199.3	−175.0
$Pd(SAF)_2Cl_2$	E^* (kJ mol^{-1})	69.5	76.6	81.9
	A (s^{-1})	2.77×10^3	7.11×10^3	2.23×10^4
	ΔS^* (JK mol^{-1})	−184.9	−177.1	−167.6
$Pd(HNAF)_2Cl_2$	E^* (kJ mol^{-1})	119.7	106.4	108.4
	A (s^{-1})	4.55×10^6	3.05×10^5	4.92×10^5
	ΔS^* (JK mol^{-1})	−124.3	−146.7	−142.8

heating weighed samples taken in porcelain crucibles on an atmosphere of air) are also included in Table 1. Kinetic parameters calculated by employing the Freeman–Carroll, the Coats–Redfern and Horowitz–Metzger equations are summarized in Table 3. The overall loss of mass from the TG curve is 86% for $Cu(SAF)_2$, 88% for $Cu(HNAF)_2$, 82% for $Pd(SAF)_2Cl_2$ and 84% for $Pd(HNAF)_2Cl_2$.

While the calculated loss in mass for these conversions are

$Cu(SAF)_2 \rightarrow CuO$	87.40%
$Cu(HNAF)_2 \rightarrow CuO$	89.1%
$Pd(SAF)_2Cl_2 \rightarrow PdO$	83.6%
$Pd(HNAF)_2Cl_2 \rightarrow PdO$	85.5%

The end products are confirmed to be CuO and PdO from their X-ray diffraction patterns.

In a recent work [10, 18], the authors studied certain transition metal chelates of the Schiff base, vanillideneanthranilic acid by TG and DTG as well as by i.r., e.p.r. and n.m.r. spectroscopy including those of copper, cobalt, nickel and zinc which are hydrated polymeric chelates. But salicylidene-2-aminofluorene chelates of cobalt(II), nickel(II), copper(II) and palladium(II) and 2-hydroxy-1-naphthalidene-2-aminofluorene chelates of copper and palladium are found to be anhydrous, based on elemental analysis, on the absence of dehydration peaks in DTG and DTA and on the absence of hydroxyl bands in i.r. spectra. Initial decomposition temperature and inflection temperature have been used to determine thermal stability of metal chelates. The initial decomposition temperature is frequently used to define the relative thermal stability of metal chelates [19].

On the basis of experimental findings in the present course of studies and the observations made by earlier workers [20, 21], the relative thermal stability of the above chelates can be given as

$$Cu(SAF)_2 \simeq Pd(SAF)_2Cl_2 \simeq Pd(HNAF)_2Cl_2 < Cu(HNAF)_2$$

Decomposition kinetics

The analysis of data using the Freeman–Carroll equation [13] and Zsakó's modified Doyle method [16] by calculation of standard deviation gives the order of the decomposition reaction near unity in all cases. Based on this value of the order of reactions, the kinetic parameters are evaluated.

The values of activation energy E^* obtained by the three methods for the four complexes are given in Table 3. The entropies of activation vary from -112 to -64 kJ^{-1} mol^{-1}. The negative values of ΔS^* in these complexes indicate that the activated complex has a more ordered structure than the reactants, and that the reactions are slower than normal [22].

Because of their similar structures all the four complexes show similar thermal behaviour, as is evidenced from their comparable values of E^* and A.

References

1 W. W. Wendlandt, Anal. Chim. Acta, 17 (1967) 428.

2 G. D. Ascenzo and W. W. Wendlandt, J. Thermal Anal., 1 (1969) 423.

3 G. C. Ascenzo and W. W. Wendlandt, Anal. Chim. Acta, 50 (1970) 79.

4 F. C. Chang and W. W. Wendlandt, Thermochim. Acta, 2 (1971) 293.

5 D. L. Perry, C. Vaz and W. W. Wendlandt, Thermochim. Acta, 9 (1974) 76.

6 C. G. Scency, J. O. Hill and R. J. Magee, Thermochim. Acta, 11 (1975) 301.

7 C. G. Scency, J. F. Smith, J. O. Hill and R. J. Magee, J. Thermal Anal., 9 (1976) 415.

8 C. K. Bhaskare, P. G. More and P. P. Hankare, Proceedings of the National Symposium on Thermal Analysis, 1981. BARC (India).

9 M. Lehtinen, Acta Pharm., Fenn., 90 (1981) 187.

10 J. Chacko and G. Parameswaran, J. Thermal Anal., 29 (1984) 3.

11 S. Vatsala and G. Parameswaran, J. Thermal Anal., 31 (1986) 883.

12 V. Indira and G. Parameswaran, Thermochim. Acta, 101 (1986) 145.

13 E. S. Freeman and B. Carroll, J. Phys. Chem., 62 (1958) 394.

14 A. W. Coats and J. P. Redgern, Nature, 201 (1964) 68.

15 H. H. Horowitz and G. Metzger, Anal. Chem., 35 (1963) 1464.

16 J. Zsakó, J. Phys. Chem., 72 (1968) 2406.

17 V. Indira and G. Parameswaran, Ind. J. Chem. 25 A (1986) 873.

18 J. Chacko, Ph. D. Thesis (1984) (Calicut University).

19 A. V. Nikolaev, V. A. Logvinenko and L. I. Myachina, Thermal Analysis, Academic Press, New York 1969, p. 779.

20 V. Sheshagiri, S. Rao and Brahmji, Z. Anal. Chim., 262 (1972) 275.

21 R. Sheshadri Naidu and R. Raghava Naidu, Ind. J. Chem., 15A (1977), 652.

22 A. A. Frost and R. G. Pearson, Kinetics and Mechanism, John Wiley and Sons, New York 1961.

Zusammenfassung — In Luft aufgenommene thermogravimetrische (TG), differentialthermogravimetrische (DTG) und differentialthermoanalytische (DTA) Kurven von CuL_2 und $Pd(LH)_2Cl_2$ (LH = Salicyliden-2-aminofluoren und 2-Hydroxy-1-naphthaliden-2-aminofluoren) werden untersucht. Aus den Massenverlusten während der Hauptschritte der Zersetzung folgt, daß die Komplexe zu den Oxiden abgebaut werden. Die mathematische Analyse der TG-Daten ergibt in allen Fällen eine Reaktionskinetik erster Ordnung. Kinetische Parameter (Energie und Entropie der Aktivierung und präexponentieller Faktor) werden angegeben.

Резюме — Методами ТГ, ДТГ и ДТА изучено в атмосфере воздуха термическое разложение комплексов CuL_2 и $Pd(LH)_2Cl_2$, где LH – салицилиден-2-аминофлуорен и 2-окси-1-нафталиден-2-аминофлуорен. Потеря веса на всех главных стадиях разложения указывает на их полное превращение до окислов. Математический анализ данных показал, что для всех случаев применим первый порядок реакционной кинетики. Приведены такие кинетические параметры, как энергия и энтропия активации и предэкспоненциальный множитель.